



Cite this: *Dalton Trans.*, 2015, **44**, 15508

## Lanthanide mixed-ligand complexes of the $[\text{Ln}(\text{CAPh})_3(\text{Phen})]$ and $[\text{La}_x\text{Eu}_{1-x}(\text{CAPh})_3(\text{Phen})]$ ( $\text{CAPh}$ = carbacylamidophosphate) type. A comparative study of their spectral properties†

Olena O. Litsis,<sup>\*a</sup> Vladimir A. Ovchynnikov,<sup>a</sup> Vasyl P. Scherbatskii,<sup>b</sup> Sergiy G. Nedilko,<sup>b</sup> Tatiana Yu. Sliva,<sup>a</sup> Viktoriya V. Dyakonenko,<sup>c</sup> Oleg V. Shishkin,<sup>c</sup> Valentine I. Davydov,<sup>d</sup> Paula Gawryszewska<sup>e</sup> and Vladimir M. Amirkhanov<sup>\*a</sup>

A series of complexes  $\text{Ln}(\text{Pip})_3(\text{Phen})$  ( $\text{Ln}(\text{III}) = \text{La, Ce-Nd, Sm-Lu, Y}$ ; HPip (CAPh type ligand) = 2,2,2-trichloro-*N*-(dipiperidin-1-yl-phosphoryl)acetamide, Phen = 1,10-phenanthroline) has been synthesized. The lanthanum(III) doped europium(III) complexes ( $[\text{La}_x\text{Eu}_{1-x}(\text{Pip})_3(\text{Phen})]$ ,  $x = 0.99, 0.95, 0.50$ ) have been obtained by the co-crystallization method. The complexes have been characterized by means of X-ray diffraction, IR,  $^1\text{H}$  and  $^{31}\text{P}$ -NMR and absorption spectroscopy. Emission and excitation luminescence spectra were recorded at 295 and 77 K. The lifetime values ( $\tau$ ) for the emission of all europium complexes were determined. The  $^5\text{D}_0$  luminescence quantum efficiency is 73–89%. The symmetries of the nearest europium surrounding in pure and doped complexes were evaluated from the Stark splitting of  $^5\text{D}_0 - ^7\text{F}_J$  transitions. Crystal structures of  $[\text{Ln}(\text{Pip})_3(\text{Phen})]$  ( $\text{Ln} = \text{Nd (1), Eu (2) and Tb (3)}$ ) have been determined. Lattice parameters of the  $[\text{Ln}(\text{Pip})_3(\text{Phen})]$  ( $\text{Ln} = \text{Tb, Yb}$ ) and the doped  $[\text{La}_x\text{Eu}_{1-x}(\text{Pip})_3(\text{Phen})]$  ( $x = 0.99, 0.95, 0.50$ ) complexes have been measured. The presence of four polymorphs within a number of rare earth elements has been estimated: two in triclinic ( $\text{Ln1} = \text{La, Nd}; \text{Ln2} = \text{Eu}$ ), one in the monoclinic ( $\text{Ln3} = \text{Tb}$ ) and one in the rhombic ( $\text{Ln4} = \text{Tb, Yb}$ ) symmetry. Complex **3** can be obtained in two crystal modifications: monoclinic and orthorhombic ones.

Received 6th July 2015,  
Accepted 22nd July 2015  
DOI: 10.1039/c5dt02557e  
[www.rsc.org/dalton](http://www.rsc.org/dalton)

## Introduction

The versatile photophysical properties of lanthanide ions have inspired vigorous research activities owing to their wide range of potential applications in the fields of lighting devices,<sup>1</sup> telecommunications<sup>2</sup> and luminescent probes for bio-analyses and live cell imaging and sensing.<sup>3</sup> Unfortunately, the molar absorption coefficients of lanthanide transitions are typically very small (less than  $10 \text{ M}^{-1} \text{ cm}^{-1}$ ). However, this weak absorbance can be overcome by coordinating to the  $\text{Ln}(\text{III})$  ion electron-rich ligands, which, upon irradiation, transfer energy to the metal center (mainly *via* the ligand triplet excited state).<sup>4</sup> Such populating of the  $\text{Ln}(\text{III})$  emitting levels is known as luminescence sensitization or the “antenna effect”.<sup>5</sup>

The light-emission characteristics of a lanthanide  $\beta$ -diketonate complex were first described by Weissman and co-workers.<sup>6</sup> Since then, numerous compounds of lanthanide ions, in particular  $\text{Eu}(\text{III})$ , with various organic ligands, have been synthesized and their crystal structures and luminescence behavior have been studied in detail.<sup>7,8</sup> However,  $\beta$ -diketonate ligands containing high-energy oscillators, such as C–H and O–H bonds, are able to quench the metal excited

<sup>a</sup>Taras Shevchenko National University of Kyiv, Inorganic Chemistry Department, 64/13, Volodymyrska Street, Kyiv 01601, Ukraine.

E-mail: olena\_litsis@mail.univ.kiev.ua, allicisster@gmail.com, vnamirkhanov@gmail.com

<sup>b</sup>Taras Shevchenko National University of Kyiv, Physics Faculty, 2, block 6, acad. Hlushkova ave., Kyiv 03680, Ukraine

<sup>c</sup>SSI “Institute for Single Crystals”, National Academy of Science of Ukraine, Lenina ave. 60, 61001 Khar’kov, Ukraine

<sup>d</sup>Taras Shevchenko National University of Kyiv, Institute of Philology, 14 Taras Shevchenko Blvd., Kyiv, Ukraine

<sup>e</sup>University of Wroclaw, Faculty of Chemistry, 14 F. Joliot-Curie Str., 50-383 Wroclaw, Poland

† Electronic supplementary information (ESI) available: Tables of elemental analysis data, IR absorption bands and their assignments, the distances of the chelate cycle atoms from the coordination bond planes and the angles around the phosphorus atom of complexes **1**, **2** and **3**. Also the ESI contains the figures of IR spectra of **1** in the solid state and in the  $\text{CHCl}_3$  solution; solid-state excitation and emission for  $[\text{Eu}(\text{Pip})_3(\text{Phen})]$  excited at 337 nm; the luminescence decay curves recorded at 77 K; the view of the  $[\text{Nd}(\text{Pip})_3(\text{Phen})]$  asymmetric unit; electronic diffuse reflection spectrum of  $[\text{Nd}(\text{Pip})_3(\text{Phen})]$  at 4 K in the 770–810 nm region. CCDC 1009969–1009971. For ESI and crystallographic data in CIF or other electronic format see DOI: 10.1039/c5dt02557e

states nonradiatively, which leads to lower luminescence intensities and shorter excited-state lifetimes. The replacement of C–H bonds with the C–Hal ones is important for the syntheses of lanthanide complexes with efficient photoemission properties.<sup>9</sup> It is well documented that the replacement of C–H bonds in a  $\beta$ -diketone ligand with lower-energy C–Hal oscillators is able to lower the vibration energy of the ligand and decreases the energy loss caused by ligand vibration and enhances the emission intensity of the lanthanide ion.<sup>10</sup> Further, due to the heavy-atom effect, which facilitates inter-system crossing, the lanthanide-centered luminescence properties are enhanced.<sup>11</sup> Substitution of carbon atoms in the (O)CCH<sub>2</sub>C(O)  $\beta$ -diketone chelating fragment can lead to increased stability of the complexes. Thus, the presence of the PO group usually provides high affinity for the majority of metal ions, and especially the rare earth (RE) elements.<sup>12</sup> This fact was also confirmed for the deprotonated  $\beta$ -diketones' structural analogues, so-called sulfonylamidophosphates (SAPH).<sup>13,14</sup> It is interesting that the substitution of the methylene group for the weak-acidic amide group allows obtaining the complexes in both molecular and acidic forms. The *N,P*-substituted  $\beta$ -diketones, so-called carbacylamidophosphates (CAPh), were selected to explore the possibility of obtaining better characteristics of lanthanide-centered luminescence of the complexes.<sup>15</sup>

Effective sensitization of the lanthanide emission was expected for the coordination compounds with 2,2,2-trichloro-*N*-(dipiperidin-1-yl-phosphoryl)acetamide (HPip),<sup>15,16</sup> Cl<sub>3</sub>CC(O)-N(H)P(O)[N(CH<sub>2</sub>)<sub>5</sub>]<sub>2</sub> which contain a chlorinated alkyl group and the additional “antenna ligand” 1,10-phenanthroline (Phen). The present work focuses on the doped lanthanide complexes' properties and is based on the systematic structure-to-property correlation investigations of the complexes with CAPh compounds.<sup>17–20</sup>

Herein, we report the synthesis and study of not only the traditional type of rare earth (RE) complexes [Ln(Pip)<sub>3</sub>(Phen)] (Ln = La, Ce–Nd, Sm–Lu, Y) but also the lanthanum doped europium ones [La<sub>x</sub>Eu<sub>1-x</sub>(Pip)<sub>3</sub>(Phen)] ( $x = 0.99, 0.95, 0.50$ ). All the coordination compounds synthesized have fully been characterized by various spectroscopic techniques. Their structural and photophysical properties have been compared with the properties of the complexes described earlier.

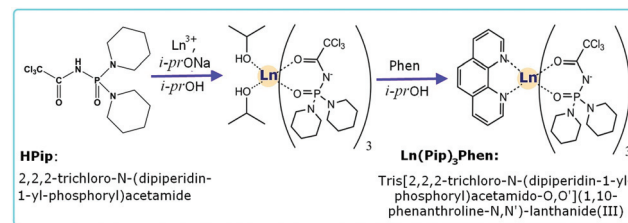
## Experimental section

### General

Ln(NO<sub>3</sub>)<sub>3</sub>·*n*H<sub>2</sub>O (Ln = La, Ce–Nd, Sm–Lu, Y) and 1,10-phenanthroline monohydrate were of “puriss. p.a.” grade and used without further purification.

2,2,2-Trichloro-*N*-(dipiperidin-1-yl-phosphoryl)acetamide (Cl<sub>3</sub>CC(O)N(H)P(O)[N(CH<sub>2</sub>)<sub>5</sub>]<sub>2</sub>, HPip), shown in Scheme 1, was prepared according to a previously described method<sup>16</sup> and was identified using IR and NMR spectroscopy.

<sup>1</sup>H and <sup>31</sup>P NMR spectra in CDCl<sub>3</sub> solutions were recorded on a Varian 400 NMR spectrometer at room temperature. <sup>1</sup>H



Scheme 1 Synthesis of [Ln(Pip)<sub>3</sub>(Phen)] complexes.

chemical shifts were determined relative to the internal standard TMS whereas <sup>31</sup>P chemical shifts were determined relative to 85% H<sub>3</sub>PO<sub>4</sub> as an external standard. Infrared (FTIR) spectra were recorded on a Perkin-Elmer Spectrum BX spectrometer using KBr pellets. The resolution of the FTIR spectra is 1 cm<sup>-1</sup>. Electronic diffuse reflectance spectra of solid samples and adsorption spectra in the UV-region were recorded on a SPECORD M-40 (Carl Zeiss, Jena) UV-Vis spectrometer with a resolution of 0.05 nm. UV-Vis absorption spectra were recorded at room temperature in absolute non-aqueous solvents on a KSVU-23 “LOMO” spectrometer using a 3 cm<sup>3</sup> stoppered quartz cell of 1 cm path length. The concentrations of the complexes were 1 × 10<sup>-3</sup> mol L<sup>-1</sup>. The resolution of the spectra was 0.05 nm in the 300–850 nm range and 0.1 nm in the 220–300 nm range. The high-resolution absorption spectra were recorded at a temperature of 4 K with a Cary 5000 UV-Vis-NIR spectrophotometer equipped with an Oxford 1204 helium flow cryostat. Elemental analyses (Ln, C, H, N) were performed using standard titrimetric methods for lanthanide ions<sup>21</sup> and the EL III Universal CHNOS elemental analyzer. The lanthanide ion concentration was determined using X-ray fluorescence (XRF) spectroscopy analysis without a reference sample on a Philips PW 1400 spectrometer with a Rh-anode tube operating at a voltage of 80 kV. The ground sample was placed on top of H<sub>3</sub>BO<sub>3</sub> (5624 mm<sup>2</sup>, Merck, 99.5%) and pressed into a pellet at 10 kbar. The luminescence measurements were performed at room temperature and 77 K using a laser spectral complex comprising various sources of exciting radiation, spectral instruments and recorders of the luminescent lighting including monochromators and lasers with 337, 473 and 532 nm wavelengths in the range of 220–575 nm. A Xe lamp (450 W) was used as the excitation source. The resolution of luminescence excitation and emission spectra was 0.05 nm.

Luminescence decay curves were recorded using the microsecond time-correlated single photon counting option of the FLS920 setup (Edinburgh Instruments Ltd). Excitation was provided by an LF900 microsecond xenon flash lamp under computer control with pulses of 1.5 to 3  $\mu$ s and an average power of >60 W up to 100 Hz and the possibility of measuring decays from 400 ns to 10 s. Luminescence decay measurements were performed in multichannel scaling mode using a TCC900 fast counter PC plug-in card. The PG900 microsecond photomultiplier gating option was used to fix the gate width and gate

**Table 1** Crystallographic data for **1**, **2** and **3**

	<b>1</b>	<b>2</b>	<b>3</b>
Empirical formula	$2(\text{C}_{48}\text{H}_{68}\text{N}_{11}\text{O}_6\text{P}_3\text{Cl}_9\text{Nd})$	$\text{C}_{48}\text{H}_{68}\text{N}_{11}\text{O}_6\text{P}_3\text{Cl}_9\text{Eu}$	$\text{C}_{48}\text{H}_{68}\text{N}_{11}\text{O}_6\text{P}_3\text{Cl}_9\text{Tb}$
Formula weight/g mol <sup>-1</sup>	2902.67	1459.05	1466.01
Wavelength/Å	0.71073	0.71073	0.71073
<i>V</i> (Å <sup>3</sup> )	6115.1(5)	3100.88(18)	6451.1(2)
<i>Z</i>	2	2	4
Temperature/K	100	100	293(2)
$\rho_{\text{calcd}}$ /mg m <sup>-3</sup>	1.576	1.563	1.50
Absorption coefficient (mm <sup>-1</sup> )	1.376	1.531	1.596
<i>F</i> (000)	2956.0	1484.0	2976.0
2θ range for data coll.	5.88–55.0	5.94–55.0	5.78–55.0
Reflection collected	51 315	27 349	55 253
Independent reflections	28 073 [ $R_{\text{int}} = 0.045$ ]	14 208 [ $R_{\text{int}} = 0.045$ ]	14 018 [ $R_{\text{int}} = 0.054$ ]
Ata/restraints/parameters	28 073/0/1405	14 208/0/703	14 018/7/731
Goodness-of-fit on <i>F</i> <sup>2</sup>	1.006	1.007	1.024
Final <i>R</i> indices [ $I > 2\sigma(I)$ ]	$R_1 = 0.0491$ , $wR_2 = 0.0918$	$R_1 = 0.0443$ , $wR_2 = 0.0794$	$R_1 = 0.0404$ , $wR_2 = 0.0677$
<i>R</i> indices (all data)	$R_1 = 0.0817$ , $wR_2 = 0.1053$	$R_1 = 0.0646$ , $wR_2 = 0.0879$	$R_1 = 0.0590$ , $wR_2 = 0.0730$
CCDC reference number	1009971	1009970	1009969

**Table 2** The unit cell parameters of the described compounds

[La(Pip) <sub>3</sub> (Phen)]	[Nd(Pip) <sub>3</sub> (Phen)] ( <b>1</b> )	[La <sub>0.5</sub> Eu <sub>0.5</sub> ]	[Eu(Pip) <sub>3</sub> (Phen)] ( <b>2</b> )	[Tb(Pip) <sub>3</sub> (Phen)] ( <b>3</b> )	[Tb(Pip) <sub>3</sub> (Phen)]	[Yb(Pip) <sub>3</sub> (Phen)]	
Crystal system	Triclinic	Triclinic	Triclinic	Triclinic	Orthorhombic	Monoclinic	Orthorhombic
Space group	<i>P</i> ī	<i>P</i> ī	<i>P</i> ī	<i>P</i> ī	<i>Pna2</i> <sub>1</sub>	<i>P</i> 2 <sub>1</sub> / <i>n</i>	<i>Pna2</i> <sub>1</sub>
<i>a</i> (Å)	15.884(19)	15.6215(8)	15.86(2)	10.9794(4)	14.6551(2)	11.49	14.5700(4)
<i>b</i> (Å)	18.55(2)	18.3288(9)	18.54(3)	13.0092(4)	17.4656(4)	43.372	17.5300(6)
<i>c</i> (Å)	23.05(3)	22.9355(11)	23.52(3)	22.3615(8)	25.2035(5)	13.963	25.0587(8)
$\alpha$ (°)	96.90(9)	97.887(4)	97.06(12)	95.215(3)	90.00	90.00	90.00
$\beta$ (°)	104.26(10)	10.38(4)	104.45(13)	97.454(3)	90.00	107.32	90.00
$\gamma$ (°)	100.10(10)	100.223(4)	100.40(13)	99.695(3)	90.00	90.00	90.00

delay, and a Hamamatsu (R928-Hamamatsu) in a Peltier-Cooled Housing was used as a detector. The photomultiplier was switched off for the duration of the exciting light flash, which ensured the removal of superimposing stray and fluorescence light.

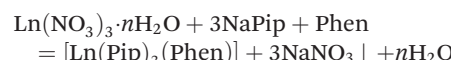
#### X-ray structure determination and refinement

Crystal data for [Nd(Pip)<sub>3</sub>(Phen)] (**1**), [Eu(Pip)<sub>3</sub>(Phen)] (**2**) and [Tb(Pip)<sub>3</sub>(Phen)] (**3**) were recorded on an Xcalibur-3 diffractometer (graphite monochromated Mo-K $\alpha$  radiation, CCD detector,  $\varphi$ - and  $\omega$ -scanning). The structures were solved by direct methods using the SHELXTL package.<sup>22</sup> Full-matrix least-squares refinement against *F*<sup>2</sup> in anisotropic approximation was used for non-hydrogen atoms. All H atoms were positioned geometrically and refined by the “riding” model with *U*<sub>iso</sub> = 1.2*U*<sub>eq</sub> of the carrier atom. CCDC 1009969–1009971 contain the supplementary crystallographic data for **1**, **2** and **3**.<sup>23</sup> Details of the data collection and refinements are given in Table 1. In the case of the isostructural crystals only unit cell dimensions were determined using the same equipment (Table 2).

## Results and discussion

### Synthesis of lanthanide complexes

[Ln(Pip)<sub>3</sub>(Phen)] (Ln = La, Ce–Nd, Sm–Lu). Tris[2,2,2-trichloro-*N*-(dipiperidin-1-yl-phosphoryl)acetamido-*O,O'*](1,10-phenanthroline-*N,N'*)-lanthanides(**III**) were synthesized according to Scheme 1.



The sodium salt of 2,2,2-trichloro-*N*-(dipiperidin-1-yl-phosphoryl)acetamide (NaPip) was prepared by the reaction between equimolar amounts of sodium isopropylate (0.069 g, 3 mmol of Na was dissolved in isopropanol) and HPip (1.129 g, 3 mmol) in an isopropanol medium and was used for the preparation of the complexes without isolation from the reaction mixture.

A solution of NaPip heated up to 55 °C (3 mmol) in isopropanol (10 ml) and 1,10-phenanthroline (0.1982 g, 1 mmol) in isopropanol (10 ml) was added to a solution of  $\text{Ln}(\text{NO}_3)_3 \cdot n\text{H}_2\text{O}$  heated up to 55 °C (1 mmol, previously it was dehydrated by *n* mmol of  $\text{HC}(\text{OC}_2\text{H}_5)_3$ ) in 10 ml acetone. After 20 minutes the resulting mixture was filtered from sodium nitrate and the filtrate was left above  $\text{CaCl}_2$  at room temperature.

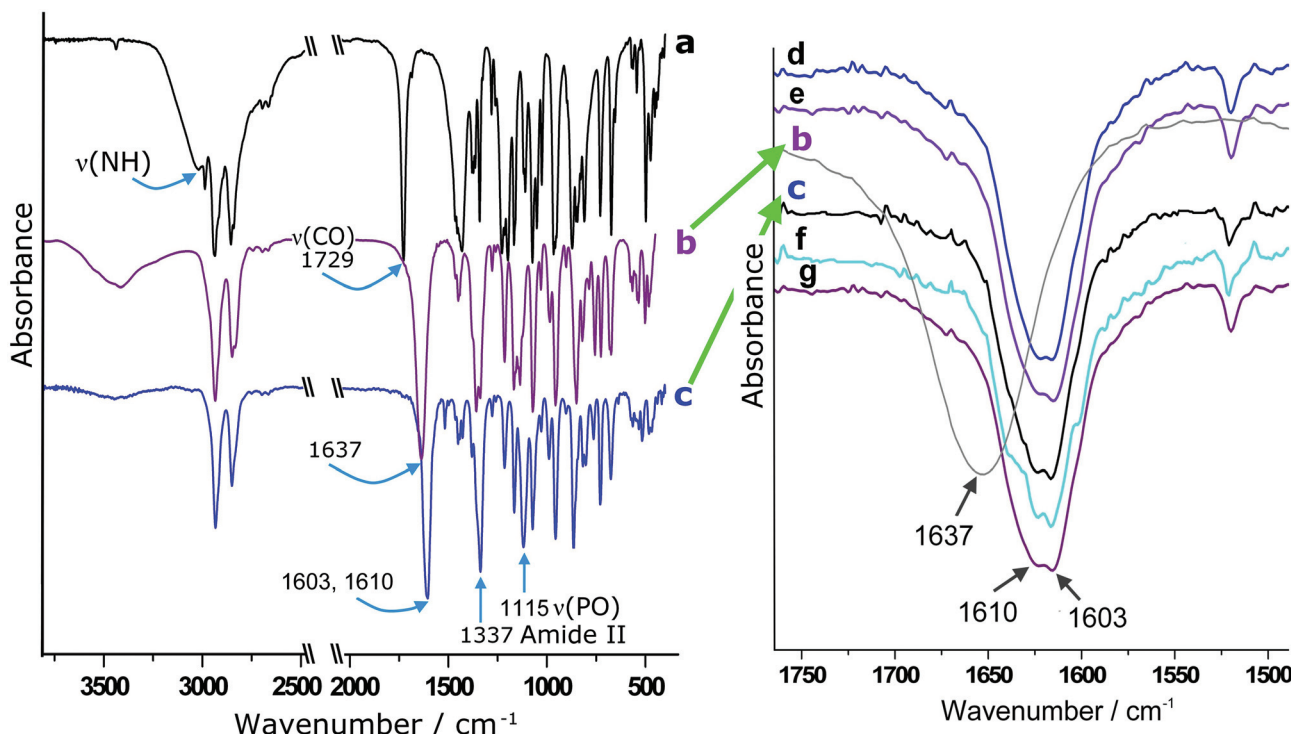


**Fig. 1** (A) FT-IR spectra of HPip (a), NaPip (b) and  $[\text{Eu}(\text{Pip})_3(\text{Phen})]$  (c); (B) the C=O stretching region in the spectra of NaPip (b),  $[\text{La}(\text{Pip})_3(\text{Phen})]$  (d),  $[\text{Nd}(\text{Pip})_3(\text{Phen})]$  (e),  $[\text{Eu}(\text{Pip})_3(\text{Phen})]$  (f),  $[\text{Tb}(\text{Pip})_3(\text{Phen})]$  (g) and  $[\text{La}_{0.5}\text{Eu}_{0.5}(\text{Pip})_3(\text{Phen})]$  (h).

The crystals of the complexes were formed after 1–2 days, filtered and washed with cool isopropanol and dried in air (yield 80–84%). The complexes, as prepared, are soluble in non-polar aprotic solvents, and are less soluble in acetone and cool alcohols. Single crystals of **1**, **2** and **3** were prepared by slow crystallization from the 2-propanol:methanol (5 : 1) mixture.

$^1\text{H}$  NMR (400 MHz, DMSO-d<sub>6</sub>, 25 °C) of  $[\text{La}(\text{Pip})_3(\text{Phen})]$ :  $\delta = 1.48$  (d, 4H <sub>$\beta$</sub> , CH<sub>2</sub>), 1.56 (d, 2H <sub>$\gamma$</sub> , CH<sub>2</sub>), 3.14 (s, 4H <sub>$\alpha$</sub> , CH<sub>2</sub>), 7.68 (m, 2H, Phen), 7.87 (m, 2H, Phen), 8.39 (d, 2H, Phen), 9.13 (d, 2H, Phen);  $[\text{Lu}(\text{Pip})_3(\text{Phen})]$ :  $\delta = 1.45$  (d, 4H <sub>$\beta$</sub> , CH<sub>2</sub>), 1.53 (d, 2H <sub>$\gamma$</sub> , CH<sub>2</sub>), 3.11 (s, 4H <sub>$\alpha$</sub> , CH<sub>2</sub>), 7.69 (m, 2H, Phen), 7.89 (m, 2H, Phen), 8.41 (d, 2H, Phen), 9.12 (d, 2H, Phen).  $^{31}\text{P}$  NMR (162 MHz, DMSO-d<sub>6</sub>, 25 °C) of  $[\text{La}(\text{Pip})_3(\text{Phen})]$ :  $\delta = 10.02$  (m);  $[\text{Lu}(\text{Pip})_3(\text{Phen})]$ :  $\delta = 11.03$ .

$[\text{La}_x\text{Eu}_{1-x}(\text{Pip})_3(\text{Phen})]$  ( $x = 0.99, 0.95, 0.50$ ). All the complexes were synthesized by the co-crystallization method according to the procedure described for  $[\text{Ln}(\text{Pip})_3(\text{Phen})]$  except that the isopropanol solution of NaPip was added to acetone solution containing stoichiometric  $\text{Eu}(\text{NO}_3)_3 \cdot 6\text{H}_2\text{O}$  and  $\text{La}(\text{NO}_3)_3 \cdot 6\text{H}_2\text{O}$ .

The compositions of the compounds based on C, H, N and titrimetric analyses are given in Table S1 (ESI<sup>†</sup>).

### Spectroscopic characterization

**FTIR spectroscopic analysis.** The IR spectra (4000–400 cm<sup>-1</sup>) of HPip and the complexes are mainly characterized

by vibrational absorptions of the phosphoryl and carbonyl groups which are sensitive to the coordination mode of the CAPh ligand.<sup>24</sup> As was shown in the previous investigations, the neutral form of CAPh coordinates mostly in a monodentate manner *via* the oxygen atom of the phosphoryl group whereas the deprotonated form coordinates in a bidentate manner *via* the oxygen atoms of the phosphoryl and carbonyl groups forming six-membered chelate cycles.<sup>15</sup> Infrared spectroscopic investigations revealed a bathochromic shift of the sodium salt NaPip and the complexes C=O and P=O stretching vibrations compared to the ligand HPip by the values of  $\Delta\nu(\text{C=O}) = 119\text{--}126\text{ cm}^{-1}$  and  $\Delta\nu(\text{P=O}) = 72\text{--}86\text{ cm}^{-1}$  (Fig. 1 and Table S2 ESI<sup>†</sup>).

The presence of a very strong band at 1603–1610 cm<sup>-1</sup> in the IR spectra of the complexes (Fig. 1) can undoubtedly be assigned to  $\nu(\text{CO})$  stretching vibrations. The C=O frequencies of all coordination compounds are close to each other. The asymmetric shape of the  $\nu(\text{CO})$  band (Fig. 1B) implies that it could be produced by an overlap of at least two bands at very close frequencies. This finding could be the evidence of the existence of similar C–O distances among the nonequivalent carbonyl groups in the complex structures. As has already been mentioned, the structures of **1**, **2** and **3** revealed different geometrical parameters of coordinated carbacylamidophosphate chelate rings within one molecule. The assumption of the crystal symmetry influence was excluded because of the vibrational bands in the spectra of all the compounds

described which preserve their shapes by dissolving in non-polar solvents (Fig. S1 ESI†). So, most probably the splitting of  $\nu(\text{CO})$  bands in the IR spectra of the complexes can be caused by non-equivalent positions of the CAPH ligands in the coordination sphere.

A broad band located at  $3027\text{ cm}^{-1}$  in the IR spectrum of HPip could be assigned to  $\nu(\text{N-H})$  of the N-H group. This band is not observed in the spectra of NaPip and the complexes, which gives evidence of a deprotonated form ( $\text{Pip}^-$ ).<sup>19,25</sup> The vibration bands of the 1,10-phenanthroline ligand in the IR spectra of the coordination compounds are overlapped by the bands of the CAPH ligands and have low intensities.

**UV/Vis spectra of  $[\text{Nd}(\text{Pip})_3(\text{Phen})]$  in solutions and in the solid state.** Lanthanide ions, as useful structural probes for biomolecular systems, have been widely studied by luminescence and absorption spectroscopy. The UV-vis absorption spectra obtained at room temperature from the solid samples of the carbacylamidophosphate ligand HPip, 1,10-phenanthroline and the coordination compounds based on them are given in Fig. 2. The HPip and Phen spectra exhibited an intense band at  $\lambda_{\text{max}}$  257 and 268 nm respectively which was attributed to a singlet–singlet  $\pi \rightarrow \pi^*$  transition. The Phen absorption band in the spectra of all the complexes was recorded at 270 nm which is very similar to the values reported for europium complexes with  $\beta$ -diketones and phenanthroline ligands<sup>26</sup> and is red shifted compared to the free ligand. The HPip absorption band is overlapped by the most intensive Phen absorptions. The orange color of the cerium complex  $[\text{Ce}(\text{Pip})_3(\text{Phen})]$  is due to the intense metal-to-ligand charge-transfer (MLCT) band at 450 nm (Fig. 2.2).<sup>27</sup>

The spectral shapes and intensities of the spectra of the solid state complexes  $[\text{La}_x\text{Eu}_{1-x}(\text{Pip})_3(\text{Phen})]$  are very similar to those of  $[\text{La}(\text{Pip})_3(\text{Phen})]$  and  $[\text{Eu}(\text{Pip})_3(\text{Phen})]$ , suggesting that

the lanthanide(III) ions do not have a significant influence on the  $\pi-\pi^*$  state energy.

Among the trivalent lanthanide ions, neodymium(III) has probably been used most frequently as an absorption probe for lanthanide–ligand interactions. The absorption band associated with  ${}^4\text{I}_{9/2} \rightarrow {}^4\text{G}_{5/2}$  and  ${}^2\text{G}_{7/2}$  transitions of Nd(III) exhibits strongly “hypersensitive” behaviour.<sup>28</sup> The intensity of these bands is mostly influenced among all the f-f transitions by the changes in the immediate surrounding of the Nd(III) ion, making it particularly suitable for probing the coordination environment around the ion. View of the spectra in the  ${}^4\text{I}_{9/2} \rightarrow {}^2\text{P}_{1/2}$  transition region indicates the splitting of the ground level in the ligand field of the Nd(III) environment.<sup>29</sup>

The electronic absorption spectra of the neodymium complex  $[\text{Nd}(\text{Pip})_3(\text{Phen})]$  (Fig. 3) show absorption features similar to those reported previously for the analogous coordination compounds having a coordination number of the central atoms of 8 with different CAPH ligands.<sup>19,30</sup> The spectra were recorded at 293 K in the 220–850 nm range in the solid state and in a diluted ( $C = 1 \times 10^{-2}$  M) chloroform solution as well (Fig. 3A and B respectively). Fig. 3 and Table 3 show the characteristic neodymium f-f transitions split by a crystal field. The precise analysis of the band splitting, mainly those of  ${}^4\text{I}_{9/2} \rightarrow {}^2\text{P}_{1/2}$  and the hypersensitive  ${}^4\text{I}_{9/2} \rightarrow {}^4\text{G}_{5/2}$ ,  ${}^2\text{G}_{7/2}$  transitions at 4 K, allows us to assume the existence of exactly one Nd(III) ion site in the structure 2. The number of components of the Kramer's doublet  ${}^4\text{I}_{9/2} \rightarrow {}^2\text{P}_{1/2}$  transition is directly related to the number of metal sites. So, only one component is observed for 2 with widths at half-height of the  ${}^4\text{I}_{9/2} \rightarrow {}^2\text{P}_{1/2}$  band of  $14.58\text{ cm}^{-1}$ . A  $J + 1/2$  number of electronic lines observed in the  ${}^4\text{I}_{9/2} \rightarrow {}^2\text{G}_{7/2}$ ,  ${}^4\text{G}_{5/2}$  transition confirms the presence of one crystallographic position of the lanthanide ion in the structure of 2 (see Fig. 3). At 4 K, additional components corresponding to the transitions from thermally

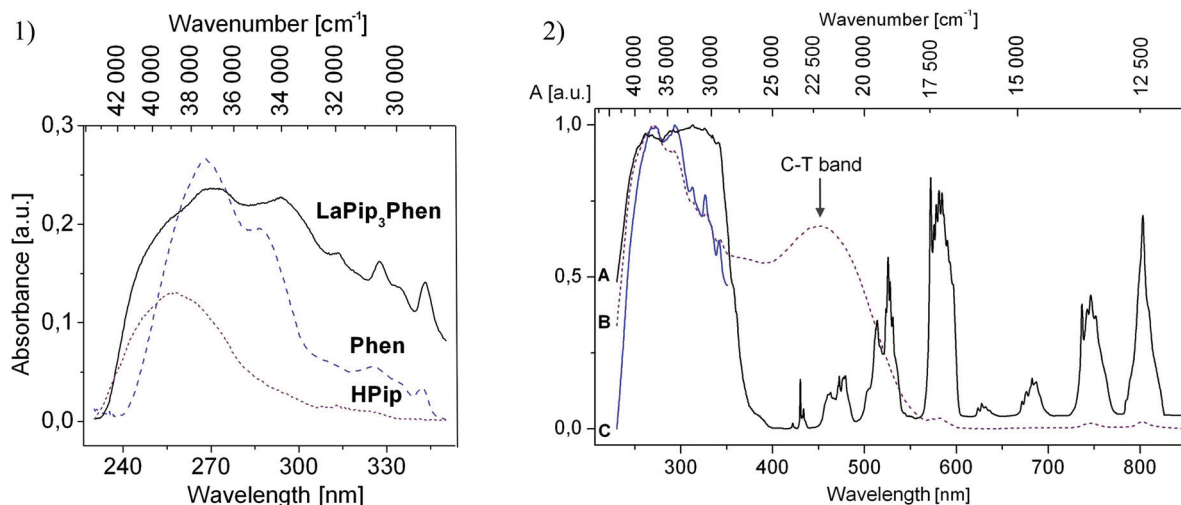


**Fig. 2** (1) Absorption spectra of organic ligands and complex  $[\text{La}(\text{Pip})_3(\text{Phen})]$  solid samples recorded under the same conditions: 0.01 g of a sample was mixed with 0.08 g of MgO at room temperature; (2) absorption spectra of solid samples of  $[\text{Nd}(\text{Pip})_3(\text{Phen})]$  (A),  $[\text{Ce}(\text{Pip})_3(\text{Phen})]$  (B) and UV region of  $[\text{La}_{0.5}\text{Eu}_{0.5}(\text{Pip})_3(\text{Phen})]$  (C) spectra recorded at room temperature.

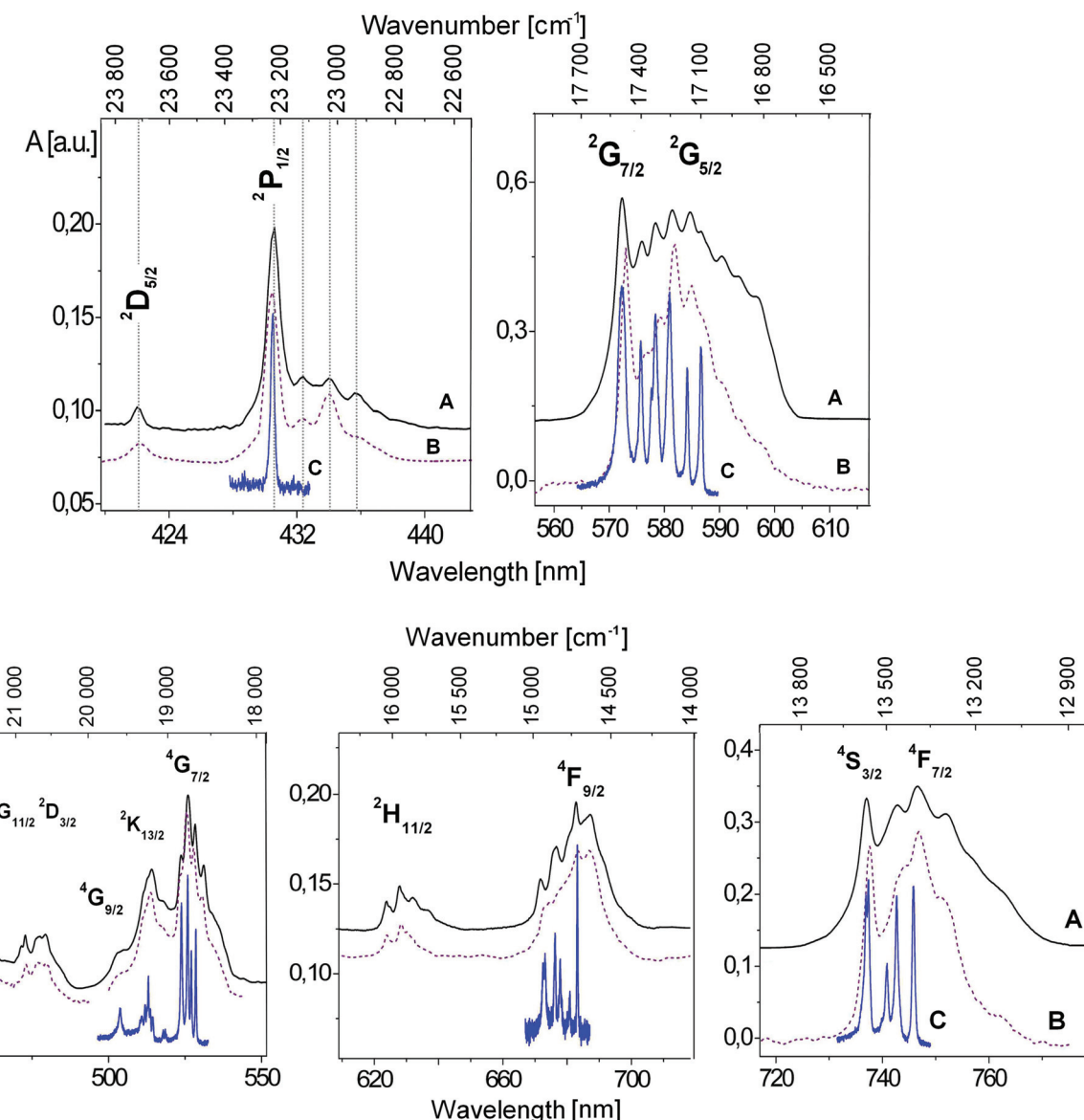


**Fig. 3** Electronic spectra of  $[\text{Nd}(\text{Pip})_3(\text{Phen})]$ : diffuse reflection spectrum at room temperature (A) and at 4 K (C); absorption spectrum of a  $1 \times 10^{-2}$  M chloroform solution (B).

populated ligand-field levels of the ground states of Nd(III) disappear from the lower energetic part of spectra, which is seen in Fig. 3A. The 4 K absorption spectra of 2 are shown in Fig. 3C. From the positions of the bands in the diffuse reflection and absorption spectra we can conclude that the coordination polyhedron in the crystalline state and in the chloroform solution has similar geometry. The shift of the most intensive band corresponding to the  $^4\text{I}_{9/2} \rightarrow ^2\text{P}_{1/2}$  transition can be attributed to the dissociation of the compound while retaining the same coordination number in the new species at the same time. This assumption was corroborated by the similarity of the absorption and diffuse reflection spectra in the hypersensitive transition region. Supplemental bands of lower intensity were observed at 430–440 nm which

can be assigned to the transitions from the upper levels of  $^4\text{I}_{9/2}$  to the singlet level  $^2\text{P}_{1/2}$ .

As was established in the previous studies,<sup>31</sup> changes in the coordination sphere of the Nd(III) ion are usually accompanied by the changes in the oscillator strength ( $P_{\text{exp}}$ ) and band shape. These parameters for the absorption in all transition regions were investigated for  $[\text{Nd}(\text{Pip})_3(\text{Phen})]$  in chloroform (Table 3, Fig. 3).

$$P_{\text{exp}} = 4.318 \times 10^{-9} \int \varepsilon(\nu) d\nu \quad (1)$$

where  $\varepsilon(\nu)$  is a molar extinction coefficient corresponding to the wavenumber  $\nu [\text{cm}^{-1}]$ .

**Table 3** Oscillator strength values  $P_{\text{exp}}$  ( $\times 10^6$ ) of f-f transitions for  $[\text{Nd}(\text{Pip})_3(\text{Phen})]$  compared to other Nd(III) complexes

S'L'J' <sup>a</sup>	Spectral range, $\text{cm}^{-1}$ (nm)	$P_{\text{exp}} (\times 10^6)$		
		Nd(Pip) <sub>3</sub> (Phen) in $\text{CHCl}_3$	NdX <sub>3</sub> (Phen) in $\text{C}_6\text{H}_{12}$ <sup>b</sup>	[Nd(acac) <sub>3</sub> (H <sub>2</sub> O) <sub>2</sub> ]·H <sub>2</sub> O in $\text{CHCl}_3$ <sup>c</sup>
<sup>4</sup> S <sub>3/2</sub> , <sup>4</sup> F <sub>7/2</sub>	12 990–13 890 (770–720)	5.73	6.26	7.07
<sup>4</sup> F <sub>9/2</sub>	14 285–15 105 (700–662)	0.62	0.69	0.48
<sup>2</sup> H <sub>11/2</sub>	15 600–16 200 (641–617)	0.11	—	0.5
<sup>4</sup> G <sub>5/2</sub> , <sup>2</sup> G <sub>7/2</sub>	16 129–17 857 (620–560)	28.15	26.49	41.53
<sup>2</sup> K <sub>13/2</sub> , <sup>4</sup> G <sub>7/2</sub> , <sup>4</sup> G <sub>9/2</sub>	18 180–20 660 (550–484)	4.01	7.59	9.01
<sup>2</sup> K <sub>15/2</sub> , <sup>2</sup> G <sub>9/2</sub> , <sup>2</sup> D <sub>3/2</sub> , <sup>4</sup> G <sub>11/2</sub>	20 410–22 730 (490–440)	1.32	1.63	1.11
<sup>2</sup> P <sub>1/2</sub>	22 730–23 500 (440–425)	0.25	0.54 <sup>d</sup>	0.20 <sup>d</sup>
<sup>2</sup> D <sub>5/2</sub>	23 500–24 200 (425–413)	0.03		

<sup>a</sup> Ref. 29. <sup>b</sup> Ref. 33. <sup>c</sup> Ref. 32. <sup>d</sup> Oscillator strength values calculated for the sum of <sup>2</sup>P<sub>1/2</sub> and <sup>2</sup>D<sub>5/2</sub> transitions.

The comparative oscillator strength values of octa-coordinated neodymium chelate complexes described earlier<sup>32,33</sup> are given in Table 3. The  $P_{\text{exp}}$  of the Nd(III) hypersensitive <sup>4</sup>I<sub>9/2</sub> → <sup>4</sup>G<sub>5/2</sub>, <sup>2</sup>G<sub>7/2</sub> transition in  $[\text{Nd}(\text{Pip})_3(\text{Phen})]$  chloroform solution spectra is similar to the ones observed in the spectra of the other complexes with carbacylamidophosphates with C.N. equal to 8 (e.g.  $[\text{NdX}_3(\text{Phen})]$  (where HX = (diethylamido)trichloroacetyl-amidophosphate,  $\text{Cl}_3\text{CC}(\text{O})(\text{N}(\text{H})\text{P}(\text{O})[\text{N}(\text{C}_2\text{H}_5)_2])_2$ ) and much less than that in  $[\text{Nd}(\text{acac})_3(\text{H}_2\text{O})_2]\cdot\text{H}_2\text{O}$  (acac = acetylacetone) complexes (Table 3). The  $P_{\text{exp}}$  values are evidence of the preferably ionic character of the metal-ligand bonds for all neodymium complexes under consideration and indicate the lowest symmetry of the octa-coordinated environment in the case of diketonate complexes containing labile H<sub>2</sub>O ligands.

The band shapes observed for  $[\text{Nd}(\text{Pip})_3(\text{Phen})]$  in the solid state and for  $[\text{Nd}(\text{Pip})_3(\text{Phen})]$  in chloroform solution allowed us to conclude that the geometry of the central atom nearest environment is the same (Fig. 3). The spectrum of the complex is similar to the eight-coordinate Nd(III) chelate.<sup>31a</sup>

### Luminescence properties of $[\text{Eu}(\text{Pip})_3\text{Phen}]$ and the doped complexes $[\text{La}_x\text{Eu}_{1-x}(\text{Pip})_3\text{Phen}]$

The solid-state photoluminescence spectra of the  $[\text{Eu}(\text{Pip})_3(\text{Phen})]$  complex and the doped complexes  $[\text{La}_x\text{Eu}_{1-x}(\text{Pip})_3(\text{Phen})]$  ( $x = 0.99, 0.95, 0.5$ ) are shown in Fig. 4 and 5. Excitation spectra were obtained by continuously monitoring the <sup>5</sup>D<sub>0</sub>–<sup>7</sup>F<sub>2</sub> transition at 610 and 613 nm respectively. The emission spectra were recorded using the excitation of lasers with 337, 473 and 532 nm wavelengths. A whole series of complexes has the highest maximum excitation wavelength at about 340 nm. The broad bands are because of the absorption by phenanthroline and CAPh ligands that clearly indicates that the ligands are acting as antennae. All the remaining much less intense narrow lines in the excitation spectra relate to f-f transitions of Eu(III) and are observed for  $[\text{Eu}(\text{Pip})_3(\text{Phen})]$  only, rather than for  $[\text{La}_x\text{Eu}_{1-x}(\text{Pip})_3(\text{Phen})]$  (Fig. 4C and D). That's why the luminescence of the doped La-Eu complexes was observed upon ligand excitation only at 337 nm laser (Fig. 4). The broad band in the excitation spectrum of  $[\text{Eu}(\text{Pip})_3(\text{Phen})]$ , arising from the absorption transition to the

ligand singlet state, is shifted to lower energies compared to the respective bands in their absorption spectra and in the excitation spectra of La-Eu compounds. This is due to the fact that the excitation is effective at the tail of the absorption band of a highly absorbing molecule, which is a consequence of the surface quenching phenomenon.<sup>34</sup> Because of the small separation between the ground state <sup>7</sup>F<sub>0</sub> and the first excited one (<sup>7</sup>F<sub>1</sub>) in europium compounds the transitions from <sup>7</sup>F<sub>1</sub> take place. Decreasing the temperature causes a reduction of the population of the first excited state of Eu(III). As a result, transitions from the <sup>7</sup>F<sub>1</sub> energy level disappear at 77 K (Fig. 2S ESI†).

The emission spectra of  $[\text{Eu}(\text{Pip})_3(\text{Phen})]$  obtained at room and liquid nitrogen temperatures by exciting the complex both through the ligand absorption transition and the europium f-f absorption transition are typical for Eu(III) compounds (line maxima at 580, 591, 610, 650 and 700 nm that originate from the <sup>5</sup>D<sub>0</sub> → <sup>7</sup>F<sub>J</sub> transitions ( $J = 0-4$ )) (Fig. 4B). Fig. 2S† presents the luminescence spectra of  $[\text{Eu}(\text{Pip})_3(\text{Phen})]$  upon laser excitation with  $\lambda_{\text{ex}} = 337$  nm at 298 and 77 K. The intense emission of the complex points to the effective energy transfer from the ligands to the emitting lanthanide levels.

The high intensity of the <sup>5</sup>D<sub>0</sub> → <sup>7</sup>F<sub>2</sub> transition having electric dipole (ED) nature compared to the allowed magnetic dipole (MD) <sup>5</sup>D<sub>0</sub> → <sup>7</sup>F<sub>1</sub> transition is in agreement with the structure determined for 2. According to X-ray data the Eu(III) polyhedra (Fig. 7) in structure 2 belonging to  $P\bar{1}$  symmetry with  $Z = 2$  have C1 site symmetry and don't have an inversion center suggesting low symmetry of charge distribution in the nearest surrounding of Eu(III) ions.<sup>7c,35</sup> The tendency for <sup>5</sup>D<sub>0</sub> → <sup>7</sup>F<sub>1</sub> and <sup>5</sup>D<sub>0</sub> → <sup>7</sup>F<sub>2</sub> Stark component degeneration at the transition from  $[\text{Eu}(\text{Pip})_3(\text{Phen})]$  to  $[\text{La}_{0.99}\text{Eu}_{0.01}]$  testifies a trend for a more symmetric distribution of effective charges around Eu(III) ions. The relative intensity of the ED to MD transition ratio can be used as a criterion for the symmetry distortion of the Eu(III) ion nearest surroundings. Among all the compounds under investigation this value is the highest in the spectrum of  $[\text{Eu}(\text{Pip})_3(\text{Phen})]$  (Table 4). It decreases gradually and becomes about two times lower in doped complexes. Judging from the spectra, the arrangement of effective charges in the surround-

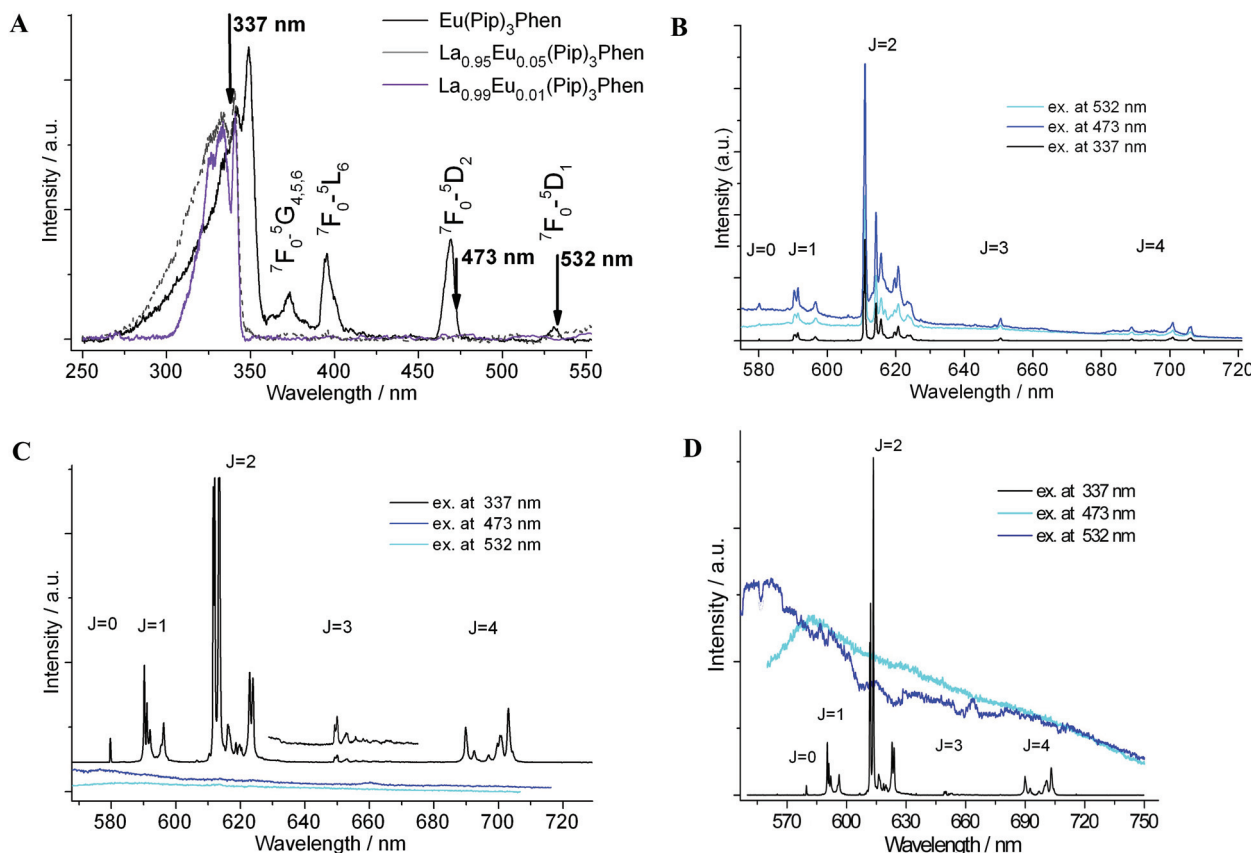


**Fig. 4** (A) Excitation spectra of the  $[\text{Eu}(\text{Pip})_3(\text{Phen})]$ ,  $[\text{La}_{0.95}\text{Eu}_{0.05}(\text{Pip})_3(\text{Phen})]$  and  $[\text{La}_{0.99}\text{Eu}_{0.01}(\text{Pip})_3(\text{Phen})]$  complexes at 77 K ( $\lambda_{\text{mon.}} = 612 \text{ nm}$ ). (B–D):  $^5\text{D}_0 \rightarrow ^7\text{F}_J$  transitions ( $J = 0–4$ ) in the luminescence spectra of  $[\text{Eu}(\text{Pip})_3(\text{Phen})]$  (B),  $[\text{La}_{0.95}\text{Eu}_{0.05}(\text{Pip})_3(\text{Phen})]$  (C) and  $[\text{La}_{0.99}\text{Eu}_{0.01}(\text{Pip})_3(\text{Phen})]$  (D) at 77 K with different wavenumbers of excitation lasers.

ings of Eu(III) ions in all doped complexes is noncentrosymmetric with a low symmetry of the crystal field.

The presence of only one sharp peak in the region of the  $^5\text{D}_0 \rightarrow ^7\text{F}_0$  transition at 580 nm and a number of Stark components for  $[\text{Eu}(\text{Pip})_3(\text{Phen})]$  (see Table 6) at 77 K testify to the presence of one luminescent center. The singlet in the region of  $^5\text{D}_0 \rightarrow ^7\text{F}_0$  transition (579.7 nm) is also observed in the emission spectra of the doped complexes  $[\text{La}_x\text{Eu}_{1-x}(\text{Pip})_3(\text{Phen})]$  (Fig. 5).

Comparison of the emission spectra for  $[\text{Eu}(\text{Pip})_3(\text{Phen})]$  and the doped La–Eu compounds shows significant differences in the shapes and the relative intensities of the transitions observed. In particular, this occurs for the hypersensitive  $^5\text{D}_0 \rightarrow ^7\text{F}_2$  transition that is sensitive to the symmetry of the coordination sphere.

The maximum number of europium f-f transition Stark components<sup>7c,29</sup> is consistent with the site symmetry of lanthanide ions close to  $C_{2v}$  in the compounds under investigation (Table 5). This result corresponds well to the X-ray data (Fig. 7). The difference in the shape of the  $[\text{Eu}(\text{Pip})_3(\text{Phen})]$  and the  $[\text{La}_x\text{Eu}_{1-x}(\text{Pip})_3(\text{Phen})]$  spectra can be explained by the belonging of the compounds investigated to different polymorph modifications.

Decay times of the  $^5\text{D}_0$  state using excitation into the ligand singlet state (337 nm) are shown in Fig. 3S (ESI†) and Table 7 for all complexes. The experimental data were fitted with  $R^2 = 0.999$  using single exponential functions, which proves the existence of only one emitting species in the complex.<sup>36</sup> The decay time of the  $[\text{Eu}(\text{Pip})_3(\text{Phen})]$  emission is temperature independent, and thus reflects the absence of thermally activated nonradiative processes, either vibrational or electronic in nature, including the  $^5\text{D}_0$  state. With the decrease of the Eu(III) concentration the emission decay time is prolonged, which can be explained by the temperature dependent triplet-triplet energy migration process<sup>37</sup> observed for all doped compounds (see Table 6). Moreover, for  $[\text{La}_{1-x}\text{Eu}_x(\text{Pip})_3(\text{Phen})]$  ( $x = 0.05$  and  $x = 0.01$ ) at 77 K a second component of the decay time of the order of 20 ms appears. This second component is related by us to the ligand phosphorescence due to the high  $[\text{La}(\text{Pip})_3(\text{Phen})]$  concentration. To confirm this the emission decay times for all europium complexes at 77 K were measured exciting the  $^5\text{D}_2$  level of the Eu(III) ion ( $\lambda_{\text{exc}} = 464.5 \text{ nm}$ ). It is found that the curves keep an exponential decay without a long-lived component with the following values: 1.61 ms ( $[\text{Eu}(\text{Pip})_3(\text{Phen})]$ ), 1.69 ( $[\text{La}_{0.95}\text{Eu}_{0.05}(\text{Pip})_3(\text{Phen})]$ ), 1.68 ms ( $[\text{La}_{0.99}\text{Eu}_{0.01}(\text{Pip})_3(\text{Phen})]$ ) and 1.71 ms ( $[\text{La}_{0.99}\text{Eu}_{0.01}(\text{Pip})_3(\text{Phen})]$ ).

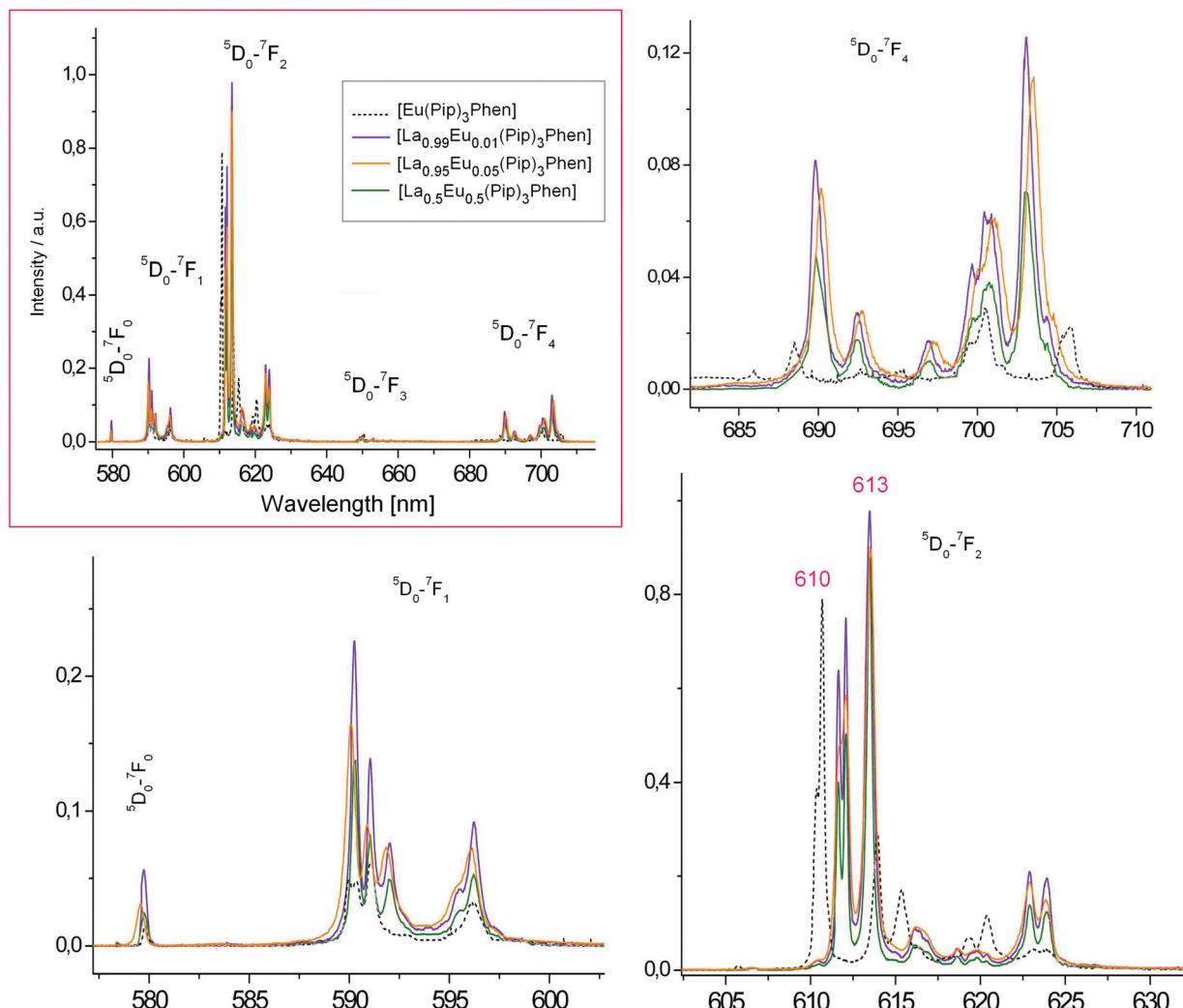


**Fig. 5** Solid-state emission spectra for  $[\text{Eu}(\text{Pip})_3(\text{Phen})]$  and  $[\text{La}_x\text{Eu}_{1-x}(\text{Pip})_3(\text{Phen})]$  excited at 337 nm at 77 K. Individual transitions in the emission spectrum are shown in the inset.

**Table 4** Relative integral intensities of  $^5\text{D}_0 \rightarrow ^7\text{F}_J$  electronic transitions in the luminescence spectra of europium carboxylates at room temperature

Compound	$^5\text{D}_0 \rightarrow ^7\text{F}_0$	$^5\text{D}_0 \rightarrow ^7\text{F}_1$	$^5\text{D}_0 \rightarrow ^7\text{F}_2$	$^5\text{D}_0 \rightarrow ^7\text{F}_3$	$^5\text{D}_0 \rightarrow ^7\text{F}_4$
$[\text{Eu}(\text{Pip})_3(\text{Phen})]$	0.045	1	8.67	0.317	1.30
$[\text{La}_{0.5}\text{Eu}_{0.5}]$	0.04	1	5.08	0.21	1.40
$[\text{La}_{0.95}\text{Eu}_{0.05}]$	0.035	1	4.56	0.091	1.126
$[\text{La}_{0.99}\text{Eu}_{0.01}]$	0.061	1	4.78	0.116	0.988

(Phen)]. The luminescence decay curves recorded at 77 K using excitation into the f-f excited state are presented in Fig. 4S (ESI†). All decay curves for the  $^5\text{D}_0$  emitting level obtained by excitation into the ligand singlet state show the

rise time. It is about two orders smaller than the decay time of the  $^5\text{D}_0$  emission indicating that the  $^5\text{D}_0$  level is populated directly from the  $^5\text{D}_1$  level. The coincidence between the temperature dependent rise time of the  $^5\text{D}_0$  emitting level and the decay time of the  $^5\text{D}_1$  excited level indicates that the energy transfer from the ligand occurs at the  $^5\text{D}_1$  level or levels above it.<sup>38</sup> The rise time of the  $^5\text{D}_0$  emitting level is not observed when the excitation is directly into the f-f excited state ( $\lambda_{\text{exc}} = 464.5$  nm).

Values of intrinsic quantum yields  $Q_{\text{Ln}}^{\text{Ln}}$  for Eu(III) are also presented in Table 6 and were calculated from lifetimes:

$$Q_{\text{Ln}}^{\text{Ln}} = \tau_{\text{obs}} / \tau_{\text{R}}$$

It was demonstrated experimentally that the radiative lifetime ( $\tau_{\text{R}}$ ) of the  $^5\text{D}_0$  excited state of Eu(III) can be calculated

**Table 5** Theoretical number of ligand-field sub-levels as a function of the  $J$  quantum number and the number of experimental splitting components<sup>7c,29</sup>

Theoretical splitting

Symmetry	Site symmetry	$J$				
		0	1	2	3	4
Cubic	$T, T_d, T_h, O, O_h$	1	1	2	3	4
Hexagonal	$C_{3h}, D_{3h}, C_6, C_{6h}, C_{6v}, D_6, D_{6h}$	1	2	3	5	6
Trigonal	$C_3, S_6, C_{3v}, D_3, D_{3d}$	1	2	3	5	6
Tetragonal	$C_4, S_4, C_{4h}, C_{4v}, D_4, D_{2d}, D_{4h}$	1	2	4	5	7
Rhombic and monoclinic	$C_1, C_S, C_2, C_{2h}, C_{2v}, D_2, D_{2h}$	1	3	5	7	9
Experimental splitting						
[Eu(Pip) <sub>3</sub> (Phen)]		1	3	4	3	8
[La <sub>0.5</sub> Eu <sub>0.5</sub> (Pip) <sub>3</sub> (Phen)]		1	5	5	3	7
[La <sub>0.95</sub> Eu <sub>0.05</sub> (Pip) <sub>3</sub> (Phen)]		1	5	5	3	7
[La <sub>0.99</sub> Eu <sub>0.01</sub> (Pip) <sub>3</sub> (Phen)]		1	5	5	3	7

**Table 6** Photophysical data for [Eu(Pip)<sub>3</sub>(Phen)] and [La<sub>x</sub>Eu<sub>1-x</sub>(Pip)<sub>3</sub>(Phen)]: observed decay time of the  $^5D_0$  state<sup>a</sup> ( $\tau_{obs}$ ), intrinsic emission quantum yield ( $Q_{Ln}^{Ln}$ ), the radiative ( $A_{rad}$ ) and nonradiative ( $A_{nrad}$ ) contributions

Compound	$\tau_{obs}/\text{ms}$		$Q_{Ln}^{Ln} (\%)$	$A_{rad} (\text{s}^{-1})$	$A_{nrad} (\text{s}^{-1})$
	295 K	77 K			
[Eu(Pip) <sub>3</sub> (Phen)]	1.58	1.55	89	564	68
[La <sub>0.5</sub> Eu <sub>0.5</sub> (Pip) <sub>3</sub> (Phen)]	1.64	2.04	63	387	222
[La <sub>0.95</sub> Eu <sub>0.05</sub> (Pip) <sub>3</sub> (Phen)]	2.03	3.83; 22.5	78	382	110
[La <sub>0.99</sub> Eu <sub>0.01</sub> (Pip) <sub>3</sub> (Phen)]	2.15	4.01; 23.6	73	341	123
EuL <sub>3</sub> Dipy <sup>b</sup>	1.65	—	57	344	262
EuL <sub>3</sub> Phen <sup>b</sup>	1.58	—	55	346	286
Na[Eu(SB) <sub>4</sub> ] <sup>c</sup>	2.32	2.52	80	345	86
Na[Eu(PMSP) <sub>4</sub> ] <sup>d</sup>	1.20	1.26	61	512	321

<sup>a</sup> The decay time values were estimated with an error of 5% ( $\lambda_{\text{exc}} = 337 \text{ nm}$ ). <sup>b</sup> These values are from: ref. 16, HL is *N*-(diphenylphosphoryl)benzamide. <sup>c</sup> Ref. 41, HPMSP is *N*-(diphenylphosphoryl)-4-methyl benzenesulfonamide,  $p\text{-CH}_3\text{C}_6\text{H}_4\text{S(O)}_2\text{NH-P(O)(C}_6\text{H}_5)_2$ . <sup>d</sup> Ref. 42, HSB is dibenzyl(phenylsulfonyl)amidophosphate.

directly from its corrected emission spectrum using the following equation<sup>39</sup>

$$1/\tau_R = A_{MD,0}\eta^3(I_{\text{tot}}/I_{MD})$$

In this formula,  $\eta$  is the refractive index of the crystal (1.5),  $A_{MD,0}$  is the spontaneous emission probability for the  $^5D_0 \rightarrow ^7F_1$  transition under vacuum ( $14.65 \text{ s}^{-1}$ ),<sup>40</sup> and  $I_{\text{tot}}/I_{MD}$  is the ratio of the total area of the corrected Eu(III) emission spectrum to the area of the  $^5D_0 \rightarrow ^7F_1$  band.

The luminescence quantum efficiency  $Q_{Ln}^{Ln}$  has the highest value for a pure Eu complex (89%) and decreases as the concentration of europium decreases. The total decay rates ( $A_{rad} + A_{nrad}$ ) are largely dominated by the radiative contribution ( $A_{rad}$ ). For all complexes the  $A_{rad}$  value decreases with the dilution when the radiative lifetime increases. It could be explained by smaller distortion of the lanthanum coordination polyhedron compared to europium due to ionic radius difference. This conclusion is similar to the ones that were made on the analysis of the ED-to-MD transition ratio.

### Description of the crystal structures

We succeeded in confirming the conclusions about the structures of the obtained compounds (based on IR and UV-Vis spectroscopy data) by the results of full X-ray analysis of the compounds [Nd(Pip)<sub>3</sub>(Phen)] (1), [Eu(Pip)<sub>3</sub>(Phen)] (2) and [Tb(Pip)<sub>3</sub>(Phen)] (3). The geometry of the complexes and the atom-labeling scheme are shown in Fig. 6–8. Selected bond lengths and angles are presented in Table S4 (ESI†) and Tables 7 and 8.

### [Eu(Pip)<sub>3</sub>(Phen)] (2) and [Tb(Pip)<sub>3</sub>(Phen)] (3)

According to the X-ray diffraction measurements the crystals of complexes 2 and 3 are not isomorphic, but they have a very similar structure (Fig. 6), and the crystals of 3 are isomorphous with [Yb(Pip)<sub>3</sub>(Phen)] crystals (Table 2).

The asymmetric unit in the crystals of 2 and 3 is created by one Ln(III) ion, three deprotonated (Pip)<sup>-</sup> ligands and one Phen coordinated molecule. Each Ln(III) ion is eight-coordinated ( $6O + 2N$ ) by three phosphoryl oxygen atoms

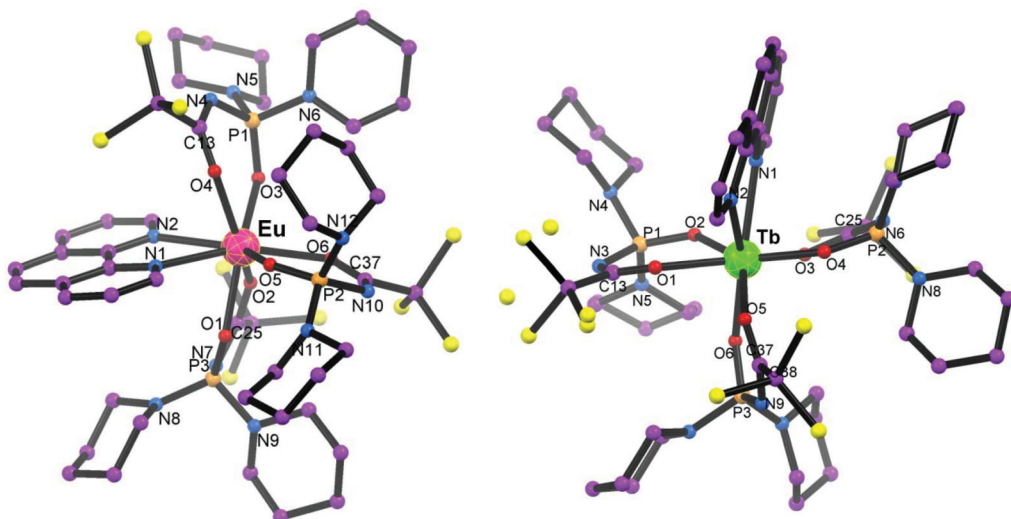


Fig. 6 Structural representation of **2** and **3** with the atom numbering scheme; H atoms are omitted for clarity.

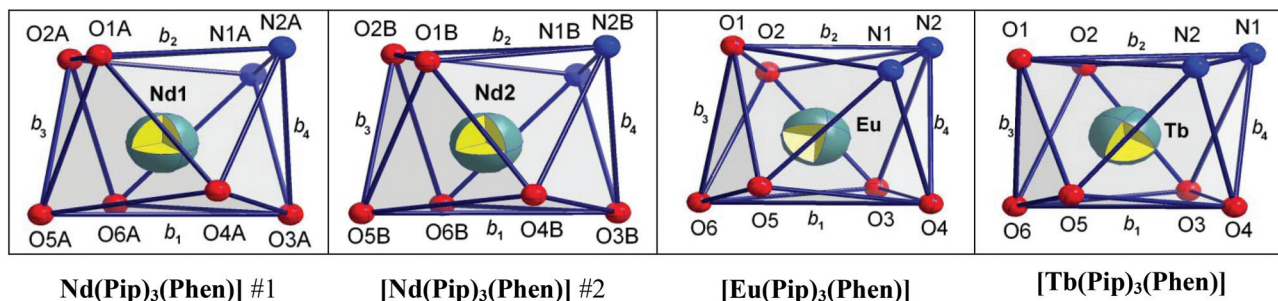


Fig. 7 The coordination polyhedra around the  $\text{Ln}(\text{III})$  central atom in complexes **1**, **2** and **3** with  $b$  parameters indicated.

(O1, O3, O5 for **2** and O2, O4, O6 for **3**), three carbonyl oxygen atoms (O2, O4, O6 for **2** and O1, O3, O5 for **3**) of three ( $\text{Pip}$ )<sup>-</sup> ligands and two nitrogen atoms (N1 and N2) of Phen (Fig. 6) with the six-membered metal chelating ring formation. The  $\text{Ln}-\text{O}$  bond lengths of the ( $\text{Pip}$ )<sup>-</sup> ligands are in the presumed range (Table 8). The  $\text{Ln}-\text{O}(\text{P})$  bonds are shorter than the  $\text{Ln}-\text{O}(\text{C})$  bonds because of stronger affinity of the phosphoryl group for lanthanides. A similar difference in bond lengths was observed for the complexes with deprotonated CAPh ligands.<sup>18,19</sup> The selected bond angles are given in Table 8. The planar bidentate chelating phenanthroline ligand is coordinated into a five-membered ring through the N1 and N2 atoms.

The Lippard–Russ and  $\delta$ -criteria were used to characterize the lanthanide ion coordination polyhedron.<sup>43</sup> The angle  $\omega$  between the nonplanar body-diagonal trapezoids O6–O5–N1–N2 and O1–O2–O3–O4 of the **2** polyhedron is equal to  $88.26^\circ$ , and that between O6–O5–N2–N1 and O1–O2–O3–O4 of the **3** polyhedron is  $-85.75^\circ$ , while in the ideal dodecahedron this angle has to be  $90^\circ$  and in the ideal antiprism  $-79.3^\circ$ .

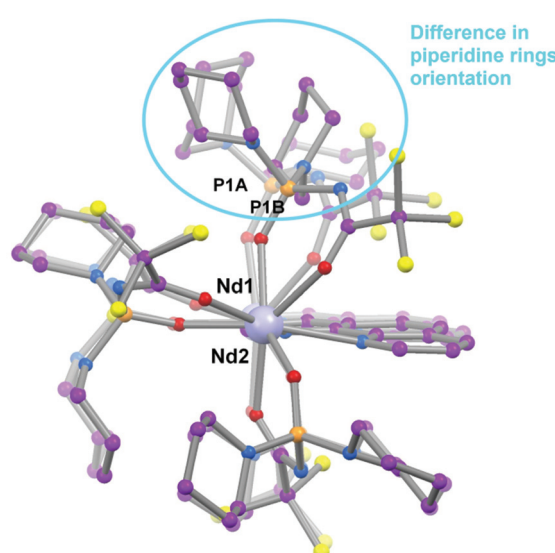


Fig. 8 Comparison of the **1**#1 and **1**#2 molecule coordinated ligand positions.

**Table 7** The criteria for determining the polyhedral shapes in the dodecahedral class and the angles  $\omega$  and  $\delta_{1-4}$  of the synthesized complexes

Polyhedron's shape	Angle, °				
	$\delta_1$	$\delta_2$	$\delta_3$	$\delta_4$	$\omega$
Hoard's dodecahedron <sup>a</sup> , $D_{2d}$	29.5	29.5	29.5	29.5	90
Bicapped trigonal prism <sup>a</sup> , $C_{2v}$	0	21.7	48.2	48.2	—
Tetragonal antiprism <sup>a</sup> , $D_{4h}$	0	0	52.5	52.5	79.3
[Nd(Pip) <sub>3</sub> (Phen)] #1	16.35	11.45	38.38	37.86	87.38
[Nd(Pip) <sub>3</sub> (Phen)] #2	12.95	17.44	42.2	41.5	87.6
[Eu(Pip) <sub>3</sub> (Phen)]	23.4	16.44	38.26	37.17	88.26
[Tb(Pip) <sub>3</sub> (Phen)]	10.46	13.91	46.08	39.24	85.75

<sup>a</sup>Theoretical polyhedron (ref. 43).

(Table 7). The set of angles  $\delta$  between the pairs of faces intersecting along the type  $b$  edges is shown in Fig. 7. The 2 and 3 polyhedra can be described as an intermediate between the bicapped trigonal prism and the tetragonal antiprism ( $C_{2v} + D_{4d}$ ), similar to the [Nd(L<sup>1</sup>)<sub>3</sub>(Phen)] mixed-ligand complex with *N,N'*-dipyrroline-*N,N'*-trichloracetylphosphortriamide ( $\text{CCl}_3\text{C(O)}\text{P(O)}[\text{N}(\text{CH}_2)_4]_2$ ) (HL<sup>1</sup>).<sup>19</sup>

The chelate (O)PNC(O) frames of all the phosphoryl ligands are planar whereas six-membered rings with the Ln central atom are far from planar, and maximum deviations from the least-squares plane are 0.31 and 0.24 Å for amide nitrogen and carbonyl oxygen atoms respectively (Table S3 ESI†). A decrease in the P–N and C–N distances in the coordinated ligand (Pip)<sup>−</sup> compared to the free ligand (Table 8) and an increase in the P=O and C=O distances demonstrate the presence of  $\pi$ -conjugation in the chelate fragments.

The phosphorus atoms of 2 and 3 have a slightly distorted tetrahedral geometry. The maximum deviation from the ideal value of 109.4° is for the NPO angle, 116.34(16) and 116.35(19)° for 2 and 3, respectively (Table S4 ESI†). It is mostly involved in the formation of six-membered chelate rings, whereas in the free ligands this angle is less than that in

the tetrahedron because of the formation of hydrogen bonds of the P=O…H–N type and equals 105.60–119.44° for HPip.<sup>16</sup> The carbonyl atom has an sp<sup>2</sup>-character.

### [Nd(Pip)<sub>3</sub>(Phen)] (1)

According to X-ray diffraction measurements the crystals of **1** are isomorphous with [La(Pip)<sub>3</sub>(Phen)] and [La<sub>0.5</sub>Eu<sub>0.5</sub>(Pip)<sub>3</sub>(Phen)] crystals (see the unit cell parameters in Table 2). A perspective view of **1**, with the numbering scheme for atoms, is displayed in Fig. 4S ESI† and 8. The asymmetric unit of the [Nd(Pip)<sub>3</sub>(Phen)] crystal structure contains two crystallographically independent molecules **1#1** and **1#2** with similar geometry. The Nd(III) ions are eight-coordinated with the primary coordination sphere made up of three (Pip)<sup>−</sup> ligands and one Phen ligand (Fig. 8). The shortest bond of neodymium is Nd1–O2A (2.360(3) Å) and Nd2–O6B (2.373(3) Å), whereas the longest is Nd1–N1A (2.673(3) Å) and Nd2–N1B (2.675(3) Å), where the oxygen atoms belong to the phosphoryl group and nitrogen to the Phen, respectively.

According to the geometrical criteria proposed for the determination of the form of the eight-apical polyhedra,<sup>43</sup> the resulting polyhedra of Nd(III) in both independent molecules of **1** can be described as an intermediate between the bicapped trigonal prism and the tetragonal antiprism,  $C_{2v} + D_{4d}$  (Table 5), similar to 2 and 3 (Fig. 7). The type of coordination by three phosphoryl oxygen atoms (O2A, O4A, O6A and O2B, O4B, O6B) and two nitrogen atoms (N1A, N2A and N1B, N2B) is the same as that for the above-presented 2 and 3 structures, with the Ln–O and Ln–N bond lengths in the assumed range. The selected bond lengths and angles with the estimated standard deviations are given in Table S6, ESI†. Deprotonation of the amide N atom in **1** changes the bond lengths in the C(O)–N–P(O) fragment with respect to that in the free ligand HPip.<sup>16</sup> The P–O and C–O bonds in **1** (Table 6) are slightly longer than the corresponding bonds in HPip. The P–N<sub>amide</sub> and C–N<sub>amide</sub> bonds are, in turn, notably shortened, which indicates resonance delocalization of the negative charge. Charge

**Table 8** Selected bond lengths (Å) in the structures HPip, **1**, **2** and **3** with the estimated standard deviations

	Ln–O(P)	Ln–O(C)	Ln–N	P=O	C=O	C–N <sub>cycle</sub>	P–N <sub>cycle</sub>	P–N <sub>term</sub> <sup>a</sup>
<b>1#1</b>	2.360(3)	2.531(3)	2.673(3)	1.500(3)	1.259(5)	1.297(5)	1.625(4)	1.651
	2.418(2)	2.439(3)	2.649(3)	1.502(3)	1.257(4)	1.295(5)	1.639(3)	1.6435
	2.380(3)	2.381(2)		1.507(3)	1.271(4)	1.281(5)	1.652(3)	1.635
<b>1#2</b>	2.390(3)	2.491(3)	2.675(3)	1.497(3)	1.250(5)	1.295(5)	1.251(4)	1.6335
	2.395(2)	2.454(3)	2.670(3)	1.504(3)	1.255(4)	1.305(5)	1.634(4)	1.638
	2.373(3)	2.392(2)		1.509(3)	1.251(4)	1.290(5)	1.631(3)	1.642
HPip <sup>b</sup>				1.4741(15)	1.200(2)	1.350(2)	1.7019(16)	1.639(2) 1.6268(16)
<b>2</b>	2.330(3)	2.467(3)	2.635(3)	1.504(3)	1.251(5)	1.255(4)	1.637(3)	1.6415
	2.363(2)	2.398(3)	2.601(3)	1.512(2)	1.264(4)	1.301(4)	1.642(3)	1.6495
	2.328(2)	2.369(2)		1.497(3)	1.255(4)	1.296(4)	1.648(3)	1.6495
<b>3</b>	2.303(3)	2.345(3)	2.589(4)	1.489(3)	1.245(5)	1.288(6)	1.613(4)	1.639
	2.315(2)	2.406(3)	2.594(4)	1.497(3)	1.235(5)	1.300(5)	1.636(4)	1.6275
	2.288(3)	2.388(3)		1.494(3)	1.244(6)	1.282(7)	1.647(3)	1.635

<sup>a</sup>For complexes these bond lengths are averaged. <sup>b</sup>Ref. 16.

redistribution from the N atom to the O atoms also affects the bond angles in the slightly distorted tetrahedral geometry around the P atom; the maximum deviation from the ideal tetrahedral value is equal to  $7.28^\circ$  for the  $\text{N}_{\text{amide}}-\text{P}-\text{O}$  angle, which is involved in the formation of a six-membered chelate ring (Table S4 ESI†). Similar tetrahedron deformations are characteristic of a majority of deprotonated CAPH complexes.<sup>18</sup> The carbonyl atoms have an  $\text{sp}^2$  character.

All of the piperidine rings of the coordinated 2,2,2-trichloro-N-(dipiperidin-1-yl-phosphoryl)acetamide are in a chair conformation. Their positions are identical in both 1#1 and 1#2 molecules, but there are different orientations of amide substituents at P1 (Fig. 8).

## Conclusions

In this contribution it has been shown that the carbacylamido-phosphate (CAPH) ligand HPip, like  $\beta$ -diketonates, forms stable heteroligand coordination compounds of the composition  $[\text{Ln}(\text{Pip})_3(\text{Phen})]$  and  $\text{Eu}^{3+}$  ions can isomorphically substitute  $\text{La}^{3+}$  in the  $[\text{La}_x\text{Eu}_{1-x}(\text{Pip})_3(\text{Phen})]$  compounds, where  $x = 0.99, 0.95$  and  $0.50$ . In the three structures studied the CAPH ligands are coordinated *via* the oxygen atoms of phosphoryl and carbonyl groups, forming six-membered cycles. Comparison of bond lengths  $\text{Ln}-\text{O}(\text{P})$  and  $\text{Ln}-\text{O}(\text{C})$  confirms the fact that the phosphoryl group has a greater affinity towards metal ions than the carbonyl one.

According to X-ray diffraction measurements the presence of four  $[\text{Ln}(\text{Pip})_3(\text{Phen})]$  polymorphs within a number of rare earth elements has been estimated: two in triclinic ( $\text{Ln}1 = \text{La, Nd}$ ;  $\text{Ln}2 = \text{Eu}$ ), one in the monoclinic ( $\text{Ln}3 = \text{Tb}$ ) and one in the rhombic ( $\text{Ln}4 = \text{Tb, Yb}$ ) symmetry. The  $[\text{La}_{0.5}\text{Eu}_{0.5}(\text{Pip})_3(\text{Phen})]$  is isomorphous with  $[\text{La}(\text{Pip})_3(\text{Phen})]$  and  $[\text{Nd}(\text{Pip})_3(\text{Phen})]$ .

The precise analysis of the absorption band splitting, mainly those of  ${}^4\text{I}_{9/2} \rightarrow {}^2\text{P}_{1/2}$  and the hypersensitive  ${}^4\text{I}_{9/2} \rightarrow {}^4\text{G}_{5/2}, {}^2\text{G}_{7/2}$  transitions of  $[\text{Nd}(\text{Pip})_3(\text{Phen})]$  at  $4\text{ K}$ , allows us to assume the existence of exactly one  $\text{Nd}(\text{III})$  ion site in this structure (there is only one component observed for 2 with widths at half-height of the  ${}^4\text{I}_{9/2} \rightarrow {}^2\text{P}_{1/2}$  band at  $14.58\text{ cm}^{-1}$ ).

The emission spectra of  $[\text{Eu}(\text{Pip})_3(\text{Phen})]$  obtained at room and liquid nitrogen temperatures by exciting the complex both through the ligand absorption transition and the europium f-f absorption transition are typical for  $\text{Eu}(\text{III})$  compounds (line maxima at  $580, 591, 610, 650$  and  $700\text{ nm}$  that originate from the  ${}^5\text{D}_0 \rightarrow {}^7\text{F}_J$  transitions ( $J = 0-4$ )). The high intensity of the  ${}^5\text{D}_0 \rightarrow {}^7\text{F}_2$  transition having electric dipole (ED) nature compared to the allowed magnetic dipole (MD)  ${}^5\text{D}_0 \rightarrow {}^7\text{F}_1$  transition is in agreement with the structure determined for 2. The tendency for  ${}^5\text{D}_0 \rightarrow {}^7\text{F}_1$  and  ${}^5\text{D}_0 \rightarrow {}^7\text{F}_2$  Stark component degeneration at the transition from  $[\text{Eu}(\text{Pip})_3(\text{Phen})]$  to  $[\text{La}_{0.99}\text{Eu}_{0.01}]$  testifies a trend for a more symmetric distribution of effective charges around  $\text{Eu}(\text{III})$  ions.

The decay times of all the europium compounds in the  ${}^5\text{D}_0$  state using excitation into the ligand singlet state ( $\lambda_{\text{exc}} =$

$337\text{ nm}$ ) and the  ${}^5\text{D}_2$  level of the  $\text{Eu}(\text{III})$  ion ( $\lambda_{\text{exc}} = 464.5\text{ nm}$ ) were determined at  $77\text{ K}$ . It was found that the decay time of the  $[\text{Eu}(\text{Pip})_3(\text{Phen})]$  emission is temperature independent in both cases. But for  $[\text{La}_{1-x}\text{Eu}_x(\text{Pip})_3(\text{Phen})]$  ( $x = 0.05$  and  $x = 0.01$ ) at  $77\text{ K}$  the second component of the decay time of the order of  $20\text{ ms}$  appears at  $337\text{ nm}$  excitation. It is related by us to the ligand phosphorescence due to the high  $[\text{La}(\text{Pip})_3(\text{Phen})]$  concentration. Applying  $\lambda_{\text{exc}} = 464.5\text{ nm}$  an exponential decay without long-lived components was observed for doped complexes with the following values of  $\tau$ :  $1.61\text{ ms}$  ( $[\text{Eu}(\text{Pip})_3(\text{Phen})]$ ),  $1.69\text{ ms}$  ( $[\text{La}_{99.5}\text{Eu}_{0.5}(\text{Pip})_3(\text{Phen})]$ ),  $1.68\text{ ms}$  ( $[\text{La}_{99.95}\text{Eu}_{0.05}(\text{Pip})_3(\text{Phen})]$ ) and  $1.71\text{ ms}$  ( $[\text{La}_{99.99}\text{Eu}_{0.01}(\text{Pip})_3(\text{Phen})]$ ).

## Acknowledgements

The authors would like to acknowledge Babaryk Artem A. and Odynets Ievgen V. (Inorganic Chemistry Department of Kyiv National Taras Shevchenko University) for carrying out X-ray fluorescence (XRF) spectroscopy analysis and X-ray diffraction measurements.

## Notes and references

- (a) A. de Bettencourt-Dias, *Dalton Trans.*, 2007, 2229–2241; (b) J.-C. G. Bünzli and C. Piguet, *Chem. Soc. Rev.*, 2005, **34**, 1048; (c) J. Kido and Y. Okamoto, *Chem. Rev.*, 2002, **102**, 2357–2368; (d) M. A. Katkova, A. G. Vitukhnovsky and M. N. Bochkarev, *Usp. Khim.*, 2005, **12**, 1193–1215.
- (a) K. Kuriki, Y. Koike and Y. Okamoto, *Chem. Rev.*, 2002, **102**, 2347; (b) A. Polman and F. C. G. M. van Veggel, *J. Opt. Soc. Am. B*, 2004, **21**, 871.
- (a) H. Tsukube, S. Shinoda and H. Tamiaki, *Chem. Rev.*, 2002, **102**, 227–234; (b) G. Mathis, *Clin. Chem.*, 1995, **9**, 1391–1397; (c) V. Fernandez-Moreira, B. Song, V. Sivagnanam, A.-S. Chauvin, C. D. B. Vandevyver, M. Gijs, I. Hemmila, H.-A. Lehr and J.-C. G. Bünzli, *Analyst*, 2010, **42**, 135.
- (a) N. V. Rusakova, V. Yu. Korovin, Z. I. Zhilina, S. V. Vodzinskii and Yu. V. Ishkov, *J. Appl. Spectrosc.*, 2004, **71**, 506–511; (b) O. V. Konnik, Z. Z. Bekirova, V. F. Shul'gin, S. B. Meshkova, P. G. Doga, S. S. Smola, G. G. Aleksandrov and I. L. Eremenko, *Russ. J. Inorg. Chem.*, 2014, **4**, 308–314; (c) S. B. Meshkova, Z. M. Topilova, N. A. Nazarenko, A. V. Litvinenko and N. P. Efryushina, *J. Anal. Chem.*, 2004, **3**, 246–249.
- (a) S. Akerboom, J. J. M. H. van den Elshout, I. Mutikainen, M. A. Siegler, W. T. Fu and E. Bouwman, *Eur. J. Inorg. Chem.*, 2013, **36**, 6137–6146; (b) J. M. Lehn, *Angew. Chem., Int. Ed. Engl.*, 1990, **29**, 1304; (c) N. Sabbatini, M. Guardiglia and J. M. Lehn, *Coord. Chem. Rev.*, 1993, **123**, 201.
- S. I. Weissman, *J. Chem. Phys.*, 1942, **10**, 214.

- 7 (a) K. Binnemans, *Chem. Rev.*, 2009, **109**, 4283–4374; (b) P. Gawryszewska, J. Sokolnicki and J. Legendziewicz, *Coord. Chem. Rev.*, 2005, **249**, 2489–2509; (c) S. V. Eliseeva and J.-C. G. Bunzli, *Chem. Soc. Rev.*, 2010, **39**, 189–227; (d) G. Vicentini, L. B. Zinner, J. Zukerman-Schpector and K. Zinner, *Coord. Chem. Rev.*, 2000, **196**, 353–382.
- 8 (a) A. R. Ramya, M. L. P. Reddy, A. H. Cowley and K. V. Vasudevan, *Inorg. Chem.*, 2010, **49**, 2407; (b) E. A. Mikhalyova, S. S. Smola, K. S. Garvilenko, V. P. Dotsenko, I. L. Eremenko and V. V. Pavlishchuk, *Theor. Exp. Chem.*, 2015, **51**, 30–36; (c) V. I. Tsaryuk, V. F. Zolin, J. Legendziewicz, R. Szostak and J. Sokolnicki, *Spectrochim. Acta, Part A*, 2005, **61**, 185–191; (d) E. A. Mikhalyova, A. V. Yakovenko, M. Zeller, M. A. Kiskin, Y. V. Kolomzarov, I. L. Eremenko, A. W. Addison and V. V. Pavlishchuk, *Inorg. Chem.*, 2015, **54**, 3125–3133.
- 9 (a) Z. M. Topilova, S. B. Meshkova, D. V. Bol'shoi, M. O. Lozinskii and Yu. E. Shapiro, *Zh. Neorg. Khim.*, 1997, **1**, 99–104; (b) S. Shubaev, V. Utochnikova, L. Marciak, A. Freidzon, I. Sinev, R. Van Deun, R. O. Freire, Y. Zubavichus, W. Grünert and N. Kuzmina, *Dalton Trans.*, 2014, **43**, 3121–3136.
- 10 (a) O. Moudam, B. C. Rowan, M. Alamiry, P. Richardson, B. S. Richards, A. C. Jones and N. Robertson, *Chem. Commun.*, 2009, 6649; (b) L.-N. Sun, J. B. Yu, G.-L. Zheng, H.-J. Zhang, Q.-G. Meng, C.-Y. Peng, L.-S. Fu and F.-Y. Liu, *Eur. J. Inorg. Chem.*, 2006, **19**, 3962; (c) D. B. Ambili Raj, S. Biju and M. L. P. Reddy, *Dalton Trans.*, 2009, 7519; (d) D. B. Ambili Raj, S. Biju and M. L. P. Reddy, *Inorg. Chem.*, 2008, **47**, 8091.
- 11 (a) N. S. Baek, M. K. Nah, Y. H. Kim and H. K. Kim, *J. Lumin.*, 2007, **127**, 707; (b) G. A. Hebbink, L. Grave, L. A. Woldering, D. N. Reinhoudt and F. C. J. M. van Veggel, *J. Phys. Chem. A*, 2003, **107**, 2483; (c) S. B. Meshkova, Yu. E. Shapiro, V. E. Kuzmin, A. G. Artemenko, N. V. Rusakova, E. G. Pykhteeva and D. V. Bolshoi, *Koord. Khim.*, 1998, **24**, 714–718.
- 12 (a) K. Gholivand, H. R. Mahzouni, M. Pourayoubi and S. Amiri, *Inorg. Chim. Acta*, 2010, **363**, 2318–2324; (b) R. V. Yizhak, K. O. Znovjyak, V. A. Ovchynnikov, T. Yu. Sliva, I. S. Konovalova, V. V. Medvediev, O. V. Shishkin and V. M. Amirkhanov, *Polyhedron*, 2013, **62**, 293–299; (c) K. Gholivand and Z. Shariatinia, *J. Organomet. Chem.*, 2006, **691**, 4215–4224.
- 13 (a) O. V. Moroz, V. A. Trush, K. O. Znovjyak, I. S. Konovalova, I. V. Omelchenko, T. Y. Sliva, O. V. Shishkin and V. M. Amirkhanov, *J. Mol. Struct.*, 2012, **1017**, 109–114; (b) K. Gubina, I. Shatrava, V. Ovchynnikov and V. Amirkhanov, *Acta Crystallogr., Sect. E: Struct. Rep. Online*, 2011, **67**, o1607; (c) O. V. Moroz, V. A. Trush, T. Y. Sliva, K. O. Znovjyak and V. M. Amirkhanov, *Acta Crystallogr., Sect. E: Struct. Rep. Online*, 2014, **6**, m209–m210.
- 14 (a) E. Kasprzycka, V. A. Trush, L. Jerzykiewicz, V. M. Amirkhanov and P. Gawryszewska, *J. Lumin.*, 2015, DOI: 10.1016/j.jlumin.2015.05.007; (b) P. Gawryszewska, O. V. Moroz, V. A. Trush, D. Kulesza and V. M. Amirkhanov, *J. Photochem. Photobiol. A*, 2011, **217**, 1–9.
- 15 V. M. Amirkhanov, V. A. Ovchynnikov, V. A. Trush, P. Gawryszewska and L. B. Jerzykiewicz, *Powerful new ligand systems: carbacylamidophosphates (CAPh) and sulfonylamidophosphates (SAPH)* // Chapter 7 in the book “*Ligands. Synthesis, Characterization and Role in Biotechnology*”, NOVA Publishers, New York, 2014, pp. 199–248.
- 16 O. O. Litsis, V. A. Ovchynnikov, S. V. Shishkina, T. Yu. Sliva and V. M. Amirkhanov, *Trans. Met. Chem.*, 2013, **38**, 473–479.
- 17 (a) O. O. Litsis, V. A. Ovchynnikov, T. Yu. Sliva, V. M. Amirkhanov, V. M. Sorokin, M. A. Minyailo, Yu. V. Kolomzarov, P. A. Tytarenko and I. E. Minakova, *Semicond. Phys., Quantum Electron. Optoelectron.*, 2013, **16**, 210–215; (b) O. V. Amirkhanov, O. V. Moroz, K. O. Znovjyak, T. Yu. Sliva, L. V. Penkova, T. Yushchenko, L. Szyrwił, I. S. Konovalova, V. V. Dyakonenko, O. V. Shishkin and V. M. Amirkhanov, *Eur. J. Inorg. Chem.*, 2014, **23**, 3720–3730; (c) K. Gubina, V. Ovchynnikov, V. Amirkhanov and S. Shishkina, *Acta Crystallogr., Sect. C: Cryst. Struct. Commun.*, 2013, **6**, 606–609.
- 18 N. S. Kariaka, V. A. Trush, T. Yu. Sliva, V. V. Dyakonenko, O. V. Shishkin and V. M. Amirkhanov, *J. Mol. Struct.*, 2014, **1068**, 71–76.
- 19 K. O. Znovjyak, O. V. Moroz, V. A. Ovchynnikov, T. Yu. Sliva, S. V. Shishkina and V. M. Amirkhanov, *Polyhedron*, 2009, **28**, 3731–3738.
- 20 S.-F. Tang, C. Lorbeer, X. Wang, P. Ghosh and A.-V. Mudring, *Inorg. Chem.*, 2014, **53**, 9027–9035.
- 21 G. Shvarcenbah and G. Flashka, *Kompleksometricheskoe titrovaniye (Complexometric titration)*, Khimiya, 1970, p. 360.
- 22 G. M. Sheldrick, *Acta Crystallogr., Sect. A: Found. Crystallogr.*, 2008, **64**, 112–122.
- 23 CCDC.
- 24 V. V. Skopenko, V. M. Amirkhanov, T. Yu. Sliva, I. S. Vasilchenko, E. L. Anpilova and A. D. Garnovskii, *Usp. Khim.*, 2004, **73**, 797.
- 25 K. E. Gubina, O. A. Maslov, E. A. Trush, V. A. Trush, V. A. Ovchynnikov, S. V. Shishkina and V. M. Amirkhanov, *Polyhedron*, 2009, **28**, 2661–2666.
- 26 S. W. Pyo, S. P. Lee, H. S. Lee, Oh. K. Kwon, H. S. Hoe, S. H. Lee, Y.-K. Ha, Y. K. Kim and J. S. Kim, *Thin Solid Films*, 2000, **363**, 232–235.
- 27 (a) R. D. Peacock and T. J. R. Weakley, *J. Chem. Soc. A*, 1971, 1937–1940; (b) A. Vogler and H. Kunkly, *Inorg. Chim. Acta*, 2006, **359**, 4130–4138.
- 28 (a) C. K. Jergensen and B. R. Judd, *Mol. Phys.*, 1964, **8**, 281; (b) G. R. Choppin, D. E. Henrie and K. Buijs, *Inorg. Chem.*, 1966, **5**, 1743; (c) R. D. Peacock, *Struct. Bonding*, 1975, **22**, 83; (d) D. E. Henrie and G. R. Choppin, *J. Chem. Phys.*, 1968, **49**, 477.
- 29 V. F. Zolin and L. G. Koreneva, *Redkozemel'nyy Zond v Khimii i Biologii [The Rare Earth Probe in Chemistry and Biology]*, Nauka, Moscow, 1980, 350, p. 123.

- 30 G. Oczko, J. Legendziewicz, V. Trush and V. Amirkhanov, *New J. Chem.*, 2003, **27**, 948–956.
- 31 (a) D. G. Karraker, *Inorg. Chem.*, 1967, **6**, 1863; (b) T. Taketatsu and C. J. Banks, *Anal. Chem.*, 1966, **38**, 1524; (c) J. Legendziewicz, K. Bukietyńska and G. Oczko, *J. Inorg. Nucl. Chem.*, 1981, **43**, 2393–2398.
- 32 A. A. Ansari, M. Irfanullah and K. Iftikhar, *Spectrochim. Acta, Part A*, 2007, **67**, 1178–1188.
- 33 V. V. Skopenko, V. M. Amirkhanov, V. A. Ovchinnikov and A. V. Turov, *Russ. J. Inorg. Chem.*, 1996, **41**, 589–594.
- 34 (a) G. Blasse, G. J. Dirksen, N. Sabbatini, S. Perathoner, J.-M. Lehn and B. Alpha, *J. Phys. Chem.*, 1988, **92**, 2419–2422; (b) J. Sokolnicki, J. Legendziewicz, G. Muller and J. P. Riehl, *Opt. Mater.*, 2005, **27**, 1529–1536.
- 35 B. Francis, D. B. A. Raj and M. L. P. Reddy, *Dalton Trans.*, 2010, **39**, 8084–8092.
- 36 H. F. Brito, O. L. Malta, L. R. Souza, J. F. S. Menezes and C. A. A. Carvalho, *J. Non-Cryst. Solids*, 1999, **247**, 129–133.
- 37 G. Blasse, G. J. Dirksen, N. Sabbatini, S. Perathoner, J. M. Lehn and B. Alpha, *J. Phys. Chem.*, 1988, **92**, 2419–2422.
- 38 W. M. Faustino, L. A. Nunes, I. A. A. Terra, M. C. F. C. Felinto, H. F. Brito and O. L. Malta, *J. Lumin.*, 2013, **137**, 269.
- 39 (a) E. B. Van der Tol, H. J. van Ramesdonk, J. W. Verhoeven, F. J. Steemers, E. G. Kerver, W. Verboom and D. N. Reinhoudt, *Chem. – Eur. J.*, 1998, **4**, 2315; (b) M. H. V. Werts, R. T. F. Jukes and J. W. Verhoeven, *Phys. Chem. Chem. Phys.*, 2002, **4**, 1542.
- 40 W. M. Faustino, O. L. Malta and G. F. de Sa, *J. Chem. Phys.*, 2005, **122**, 054109.
- 41 P. Gawryszewska, O. V. Moroz, V. Trush, V. M. Amirkhanov, T. Lis, M. Sobczyk and M. Siczek, *ChemPlusChem*, 2012, **77**, 482.
- 42 E. Kasprzycka, V. A. Trush, V. M. Amirkhanov, L. Jerzykiewicz and P. Gawryszewska, *Opt. Mater.*, 2014, **37**, 476–482.
- 43 M. A. Porai-Koshits and L. A. Aslanov, *J. Struct. Chem.*, 1972, **13**, 244–253.